Published online 10 April 2019 *Nucleic Acids Research, 2019, Vol. 47, No. 11* ***5723–5734***
doi: 10.1093/nar/gkz249

Replicative DNA polymerases promote active displacement of SSB proteins during lagging strand synthesis

Fernando Cerrón[1,2], Sara de Lorenzo[1], Kateryna M. Lemishko[1,3], Grzegorz L. Ciesielski[4], Laurie S. Kaguni[4], Francisco J. Cao[1,2,*] and Borja Ibarra[1,3,*]

[1]Instituto Madrileño de Estudios Avanzados en Nanociencia, IMDEA Nanociencia. 28049 Madrid, Spain, [2]Departamento Estructura de la Materia, Física Térmica y Electrónica. Universidad Complutense. 28040 Madrid, Spain, [3]Instituto Madrileño de Estudios Avanzados en Nanociencia (IMDEA Nanociencia) & CNB-CSIC-IMDEA Nanociencia Associated Unit "Unidad de Nanobiotecnología". 28049 Madrid, Spain and [4]Department of Biochemistry and Molecular Biology and Center for Mitochondrial Science and Medicine, Michigan State University, East Lansing, MI 48823, USA

Received November 02, 2018; Revised March 22, 2019; Editorial Decision March 25, 2019; Accepted March 29, 2019

ABSTRACT

Genome replication induces the generation of large stretches of single-stranded DNA (ssDNA) intermediates that are rapidly protected by single-stranded DNA-binding (SSB) proteins. To date, the mechanism by which tightly bound SSBs are removed from ssDNA by the lagging strand DNA polymerase without compromising the advance of the replication fork remains unresolved. Here, we aimed to address this question by measuring, with optical tweezers, the real-time replication kinetics of the human mitochondrial and bacteriophage T7 DNA polymerases on free-ssDNA, in comparison with ssDNA covered with homologous and non-homologous SSBs under mechanical tension. We find important differences between the force dependencies of the instantaneous replication rates of each polymerase on different substrates. Modeling of the data supports a mechanism in which strong, specific polymerase-SSB interactions, up to ∼12 k_BT, are required for the polymerase to dislodge SSB from the template without compromising its instantaneous replication rate, even under stress conditions that may affect SSB–DNA organization and/or polymerase–SSB communication. Upon interaction, the elimination of template secondary structure by SSB binding facilitates the maximum replication rate of the lagging strand polymerase. In contrast, in the absence of polymerase–SSB interactions, SSB poses an effective barrier for the advance of the polymerase, slowing down DNA synthesis.

INTRODUCTION

Genome duplication induces the formation of transient single-stranded DNA (ssDNA) intermediates, usually thousands of nucleotides long, which are rapidly covered by single-stranded DNA-binding (SSB) proteins. SSBs bind ssDNA in a sequence-independent manner with high affinity, generally in the picomolar range (1–4). SSB binding protects ssDNA from degradation and greatly stimulates DNA replication *in vitro*. This stimulation is in part due to the many roles attributed to SSBs (reviewed in (1,2,4)), such as prevention of ssDNA degradation, removal of ssDNA secondary structure, increased primer recognition and initiation, decreased non-specific binding of DNA polymerase to the template, and stimulation of the average primer extension and strand displacement activities of the DNA polymerase. Due to their many functions during DNA replication, SSBs are found in all organisms, and are absolutely required for the synthesis of genomic and mitochondrial DNA.

In humans, the replication mechanism of mitochondrial DNA remains actively debated, though increasing experimental evidence indicates that during replication of the L-strand (equivalent to the lagging strand of nuclear DNA), the mitochondrial replicase, Polγ, works on long stretches of ssDNA intermediates covered by mitochondrial SSB, mtSSB (5–9). Human mtSSB has significant sequence and structural homology (10,11) with the well-characterized

*To whom correspondence should be addressed. Tel: +34 912998863; Email: borja.ibarra@imdea.org
Correspondence may also be addressed to Francisco J. Cao. Tel: +34 91 394 4742; Email: francao@fis.ucm.es
Present addresses:
Fernando Cerrón, Hospital Universitario de Canarias. 38320 Santa Cruz de Tenerife, Spain.
Grzegorz L. Ciesielski, Department of Chemistry, Auburn University at Montgomery, Montgomery, AL 36117, USA.

SSB from *Escherichia coli* (EcoSSB). Sequence comparison showed that the major differences between these two proteins are that residues 1–9 and 55–59 of mtSSB are missing in EcoSSB and that EcoSSB contains an additional C-terminal tail missing in mtSSB (11). Apart from these differences, these two SSBs share fast binding (10^9–10^{11} M^{-1} s^{-1}) and slow dissociation (10^{-1}–10^{-2} s^{-1}) kinetics to and from ssDNA (12,13) and bind preformed ssDNA as tetramers in at least two different modes. In each mode, ∼30 ($mtSSB_{30}$) or ∼60 ($mtSSB_{60}$) nucleotides are organized per tetramer depending on the salt and protein concentrations (3,12–14). In fact, both proteins stimulate *in vitro* the primer extension activity of Polγ (15,16). Interestingly, biochemical and physiological studies showed that a mtSSB variant ($mtSSB_{2,3}$) carrying a deletion of amino acids 51–59 (those missing in EcoSSB) stimulates the activity of Polγ less than wild-type mtSSB (17). These nine amino-acids pertain to loop 2.3, which is a flexible domain characteristic of vertebrate mtSSBs. The loop 2.3 is located on the surface of mtSSB close to the ssDNA-binding channel but is not involved in ssDNA binding. These findings suggest that specific structural elements of mtSSB may play a role in facilitating the primer extension activity of Polγ (i.e. via species-specific interactions).

To date, several questions remain unanswered about how apparently competing functions of polymerase and SSB are coordinated during synthesis of the lagging strand. First, the mechanism by which replicative DNA polymerases dislodge the long-lived SSB–DNA complexes in a manner that does not compromise the advance of the replication fork is unknown. This is a remarkable task considering that during lagging strand synthesis the high density of SSB bound to the template would restrict the capacity of a single SSB to diffuse (18,19), and the absence of free ssDNA ends would prevent SSB from being pushed outward by the advance of the polymerase (20). Second, the nature of the stimulatory effect of SSB on the average replication velocity described in bulk studies is not known. Is stimulation due to direct polymerase–SSB connections, which enhance the instantaneous primer extension rate of the polymerase? Or instead, is it due to an indirect role of SSB in the organization of the template?

Here, we aimed to answer these questions using optical tweezers to determine the coordinated action of human mtSSB and Polγ, in a single-molecule assay mimicking lagging strand synthesis under different mechanical tensions. Mechanical tension applied to the ends of ssDNA modulates the replication rate of DNA polymerases (21–26), and when applied to the ends of ssDNA–SSB complexes, it regulates the binding modes of SSB proteins (14,27,28). Consequently, mechanical tension can be employed as a useful variable to determine the mechanistic processes involved in the replication of SSB–DNA complexes, and to quantify the energies involved in the mechanism of SSB release by DNA polymerases.

In our studies, we measured and compared the real-time kinetics of individual Polγ holoenzymes replicating under mechanical tension either free-ssDNA or ssDNA covered by either human wild-type mtSSB ($mtSSB_{WT}$), the mtSSB variant $mtSSB_{2,3}$ or EcoSSB. In order to explore whether our findings can be extended to other DNA replication systems, we also measured the effect of bacteriophage T7 SSB (gp2.5), $mtSSB_{WT}$ and EcoSSB on the instantaneous replication rate of the T7 DNA polymerase (T7DNAp) under mechanical tension. Interestingly, the two DNA polymerases under study responded similarly to the absence or presence of homologous and non-homologous SSBs in the template: For both DNA polymerases, the instantaneous replication rate increased rapidly with tension (<6 pN), when DNA synthesis occurred on free-ssDNA. In contrast, in the presence of their homologous SSBs, both polymerases replicated at their maximum rates within the entire range of tension at which SSB remained stably bound to the template (<8 pN). Interestingly, non-homologous or mutant SSBs covering the DNA template prevented both DNA polymerases from achieving their maximum replication rates. Overall, these results are compatible with a model in which the secondary structure of free DNA presents a significant barrier (∼2 k_BT) to the advance of these replicative DNA polymerases. Destabilization of the secondary structure by SSB binding favored maximum instantaneous replication rates but only when functional interactions between polymerase and SSB promoting SSB release are established. In particular, for the mitochondrial replication proteins we found that specific polymerase–SSB interactions, as high as ∼12 k_BT (22°C) between residues of loop2.3 of mtSSB and Polγ, allow this polymerase to displace the SSB tetramers from the template without hindering its replication rate, even under mechanical stress conditions that affect the SSB–DNA structure. The similarities found in the mitochondrial and bacteriophage T7 DNA replication systems suggest that their respective polymerases may use similar mechanisms to dislodge the tightly bound SSBs during lagging strand DNA synthesis.

MATERIALS AND METHODS

Proteins and DNA constructs

Recombinant $mtSSB_{WT}$ and $mtSSB_{2,3}$ proteins were prepared from bacterial cells as described previously (15). Recombinant catalytic and accessory subunits of human Polγ were prepared from S*f*9 and bacterial cells, respectively, as described previously and combined in a 1:1.5 molar ratio to reconstitute the holoenzyme (29). Recombinant EcoSSB was purchased from Thermofisher and recombinant T7 DNAp and gp2.5 were purchased from New England Biolabs and LSBio, respectively. The gapped DNA template, consisting of ∼900 nt of ssDNA flanked by ∼3550 bp ds-DNA handles, was prepared from *pBacgus*11 vector (Novagen) and labeled with digoxigenin (Dig) at one end and biotin at the other, as described in (21). The approximate length of the ssDNA fragment was determined by denaturing gel electrophoresis (Supplementary Figure S1).

Optical tweezers experiments

We used a counter propagating dual-beam optical tweezers instrument to manipulate individual DNA molecules (30). Data were monitored at 500 Hz at 22 ± 1°C.

SSB-free and SSB-bound ssDNA force–extension curves (FECs). ssDNA was obtained by unzipping mechanically

a dsDNA hairpin of 510 bp (31) using the oligonucleotide hybridization method described previously, Supplementary Figure S2 (14). SSB proteins were introduced inside the flow cell after dilution to 50 nM (or 100 nM for gp2.5) in the replication buffer without dNTPs: 50 mM Tris pH 8.5, 30 mM KCl, 10 mM Dithiothreitol (DTT), 4 mM $MgCl_2$, 0.2 mg/ml bovine serum albumin. SSB binding to preformed ssDNA was carried out at constant tensions <8 pN. Once equilibrium was reached, tension was varied with a constant pulling rate of 150 nm s^{-1}, in order to obtain the final FEC of each SSB–DNA complex. A minimum of 5 FECs were obtained for ssDNA and for each SSB–DNA complex.

Primer extension activities. A gapped DNA molecule was tethered between an anti-Dig and streptavidin covered beads. Polγ and T7DNAp were introduced inside the flow cell diluted to 2 nM (unless otherwise indicated) in the replication buffer containing the four dNTPs (50 μM). Individual replication traces were obtained in free or SSB-covered gapped-DNA substrates. SSB concentration was 50 nM in all cases except for gp2.5, which was 100 nM. Data were taken in the 'constant force feedback' mode. In this mode, the distance between the beads was adjusted to maintain a constant tension in the DNA as the single-stranded template is replicated to dsDNA.

Data analysis

Secondary structure. The amount of secondary structure in ssDNA as a function of mechanical tension was quantified from experimental FECs of ssDNA (Figure 1C) according to Bosco *et al.* (32), Supplementary Figure S3.

SSB-binding mode and protein coverage determination. The binding mode (number of nucleotides wrapped per SSB tetramer) and protein coverage (the fraction of the ssDNA covered by SSB) of mtSSB and EcoSSB were determined from experimental ssDNA–SSB FECs according to a phenomenological model described previously (33), Supplementary Figure S2.

ΔG_{SSB} *calculation.* The average Gibbs energy to unwrap one nucleotide from an SSB tetramer at a specific force value was calculated by integrating the area between the FECs of the SSB-bound and SSB-free ssDNA above that specific force (Supplementary Figure S2). The area was divided by the total number of nucleotides and corrected by the protein coverage. The change of ΔG_{SSB} with force for $mtSSB_{WT}$, $mtSSB_{2.3}$ and EcoSSB are shown in Supplementary Figure S2D.

Average velocity and processivity. The number of nucleotides incorporated by Polγ and T7DNAp was obtained by dividing the distance change between the beads by the change in extension at a given force accompanying the conversion of one SSB-free, or SSB-bound, single-stranded nucleotide into its double-stranded counterpart. The average extensions of SSB-free and SSB-bound ssDNA nucleotides as a function of force are shown in Figure 1C. The dsDNA was approximated with the worm-like chain model for polymer elasticity with a persistent length of $P = 53$ nm and stretch modulus $S = 1200$ pN/nm (34). The average replication rates at each tension were determined by a line fit to the traces showing the number of replicated nucleotides versus time. The final rate at each tension was obtained by averaging over all of the traces taken at similar tension values (±1 pN).

V_{max} *identification.* The instantaneous replication rate without pauses was determined with an algorithm that computes the instantaneous velocities of the trajectory, averaging the position of the enzyme in the template over sliding time windows. A detailed description of the method and its validation with simulated replication traces, mimicking conditions found in experimental traces, is provided in Supplementary Data and Supplementary Figure S4.

RESULTS

Detection of Polγ individual replication activities and determination of SSB–ssDNA force–extension curves

We used a highly stable, miniaturized optical tweezers device (30) to investigate the real-time kinetics of individual Polγ molecules replicating a gapped DNA molecule containing a ∼900 nt ssDNA segment flanked by ∼3550 bp dsDNA handles attached between two micro-sized beads ('Materials and Methods' section). One bead is held in the optical trap and the other on top of a micropipette (Figure 1A). We monitored at constant force, from ∼1 to 17 pN, the end-to-end distance change of the DNA construct (Δx in Figure 1A) as Polγ converts to dsDNA the ssDNA segment, either not covered or covered *in-situ* by $mtSSB_{WT}$, $mtSSB_{2,3}$ or EcoSSB proteins (Figure 1B and 'Materials and Methods' section). Experiments were performed at salt conditions appropriate for DNA synthesis (30 mM KCl and 4 mM $MgCl_2$) (14,17) and at 50 nM SSB concentration (for all three SSB proteins). These conditions are known to favor the low binding site-size mode of $mtSSB_{WT}$ and EcoSSB (1,3,13,14), which has been recently shown to represent the binding mode selected preferentially during the process of DNA replication (14). Indeed, analysis of the force–extension curves (FECs) of the three SSB–DNA complexes (Figure 1C) indicated that under these conditions all three SSBs bind to ssDNA in the low site-size mode (∼30 nt/ tetramer) and cover 80–90% of the template at tensions below 8 pN, Supplementary Figure S2 (33). Above this tension, we and others have shown that force promotes significant ssDNA unwrapping from SSB, leading to release of the protein from the template (14,28).

Template secondary structure hinders the instantaneous replication rate by Polγ

We first aimed to characterize the real-time kinetics of Polγ on SSB-free ssDNA under mechanical tension. Analysis of independent replication traces of Polγ on ssDNA ($N = 100$) showed that at the lowest tensions (∼1 pN) the average number of nucleotides (nt) incorporated was 450 ± 25 nt (processivity), and the average rate of DNA synthesis was 6 ± 1 nt s^{-1} (Supplementary Figure S5). These values are in good agreement with the average processivity, ∼560 nt and average primer extension rate, ∼6 nt s^{-1} described *in vitro*

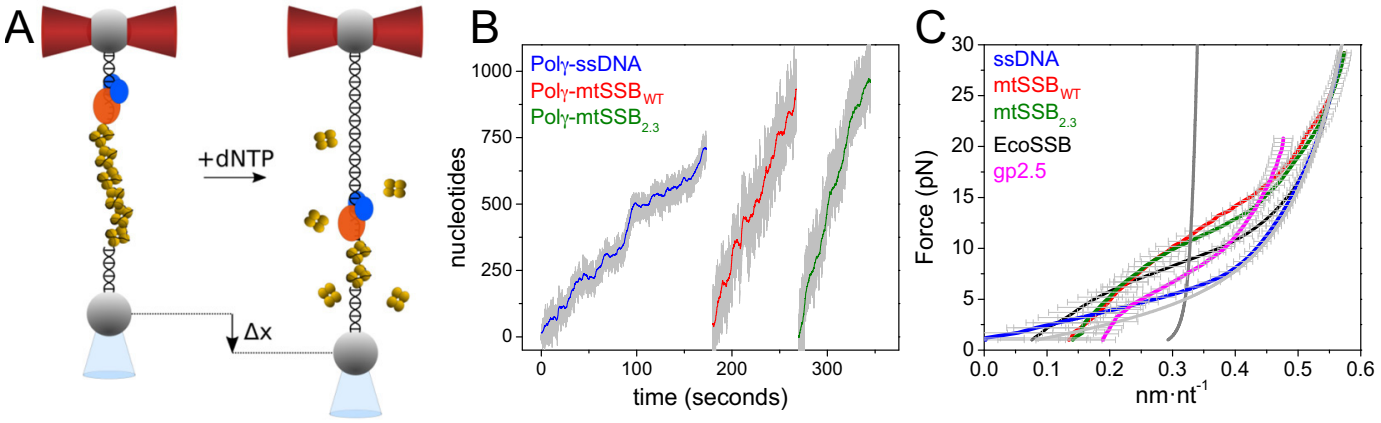

Figure 1. Individual replication activities and SSB–ssDNA FECs. (**A**) Experimental setup to measure individual replication activities in the presence of SSB. A single DNA molecule containing a ssDNA gap (∼900 nt) was tethered between two beads: one held in the optical trap (red cone) and the other on top of a micropipette (in light blue). SSB (golden) binds to the template and the DNA polymerase (blue-red) loads at the 3′ end of the primer-template. In the presence of dNTPs, the polymerase starts DNA synthesis, releasing SSBs as it advances along the template. At constant force below ∼10 pN, the activity of the polymerase increases the distance between the beads (Δx). (**B**) Representative replication traces of Polγ obtained at constant tension of 1 pN on SSB-free ssDNA (blue) and ssDNA covered with mtSSB$_{WT}$ (red) or mtSSB$_{2.3}$ (green). Raw data (gray) were filtered within 3 s. Traces were shifted along the time axis for clarity of display. (**C**) Average FECs of SSB-free ssDNA (blue) and ssDNA covered with either mtSSB$_{WT}$ (red), mtSSB$_{2.3}$ (green), EcoSSB (black) or gp2.5 (magenta) in replication buffer ('Materials and Methods' section). Dark gray line: Worm-Like-Chain (WLC) model for dsDNA elasticity (persistence length, $P = 0.34$ nm, stretch modulus, $S = 1200$ pN). Light gray line: WLC model for ssDNA elasticity ($P = 0.7$ nm, $S = 800$ pN). Each FEC corresponds to the average of at least five independent curves. Error bars show standard error..

for the reconstituted human holoenzyme under similar salt conditions (6,15,35,36). Polymerase concentration was kept low (2 nM) to ensure that each DNA synthesis event corresponds to the activity of a single holoenzyme. The time interval between synthesis events was typically about 10 times larger than the duration of a single event. In addition, varying the polymerase concentration 50-fold (from 0.2 to 10 nM) did not change significantly either the average replication velocity or the processivity (Supplementary Figure S6). These observations suggest that each replication run corresponds to the activity of a single polymerase.

We developed a new method ('velocity prominence' method) to calculate the average replication rate without pauses, V_{max}, from molecular motor trajectories presenting slow average moving rates, such as Polγ (Supplementary Data and Supplementary Figure S4). Validation of the method on simulated traces (as described in 37) indicated that V_{max} values reported for our experimental data may present an average underestimation of ∼13% (Supplementary Data). Analysis of V_{max} showed that in SSB-free ssDNA V_{max} depends strongly on the tension applied to the template: V_{max} increased with tension <6 pN, from ∼15 to 25 nt s^{-1}, to gradually decrease toward stalling at tensions >6 pN (Figure 2A). Similar dependencies of the replication rate on tension have been described for other replicative DNA polymerases (23–26). The activity of Polγ, as with majority of replicative DNA polymerases, is hampered by stable secondary structure of the template (38–40). Accordingly, we noticed that Polγ reaches its maximum replication rate at ∼6 pN, which is the tension value that promotes the destabilization of ∼100% of the template secondary structure under our experimental conditions ('Materials and Methods' section and Supplementary Figure S3).

Based on these observations, we considered that V_{max} is modulated by the work to convert a single-stranded nucleotide to double-stranded form, plus the work required to disrupt the secondary structure characteristic of free-ssDNA at each tension. We thus fit the measured force–velocity data to the Arrhenius law (41):

$$V_{max}(f) = k(0)\exp(-[\delta \cdot f \cdot (x_{ss}(f) - x_{ds}(f)) + \Delta G_{eff} \cdot (1 - \varphi(f))]/k_B T) \quad (1)$$

The free-variables in this model are: $k(0)$, which is the replication rate at zero tension ($f = 0$ pN) in the absence of template secondary structure and ΔG_{eff}, or the average energy barrier imposed by the template secondary structure on the advance of the polymerase. The parameter δ defines the kinetic step size of the DNA polymerase and was fixed to 1 nt/ step, according to bulk, structural and single-molecule data (42–45). The fraction of ssDNA template bases forming secondary structure as a function of force, $(1 - \varphi(f))$, together with the lengths of single- and double-stranded nucleotides at each tension ($x_{ss}(f)$ and $x_{ds}(f)$, respectively), were quantified from experimental FECs ('Materials and Methods' section and Figure 1C; Supplementary Figure S3), k_B is the Boltzmann constant and T the absolute temperature. Equation (1) was fitted to data (Figure 2A) minimizing the mean square difference given for the two free parameters; $k(0) = 23.0 \pm 0.7$ nt s^{-1} and $\Delta G_{eff} = 1.4 \pm 0.2\ k_B T$ (Table 1). The value of $k(0)$ matches the intrinsic nucleotide incorporation rates determined previously *in vitro* for *Drosophila melanogaster*, 15 nt s^{-1} and human, 37 nt s^{-1} mitochondrial DNA polymerases (46–48). The model points out the important role of the salt-stabilized template secondary structure on modulating the replication rate at low tensions (i.e. it represents an effective barrier of ∼1.4 $k_B T$ for Polγ under the current experimental conditions). Below 6 pN, the initial increase in the replication rate is

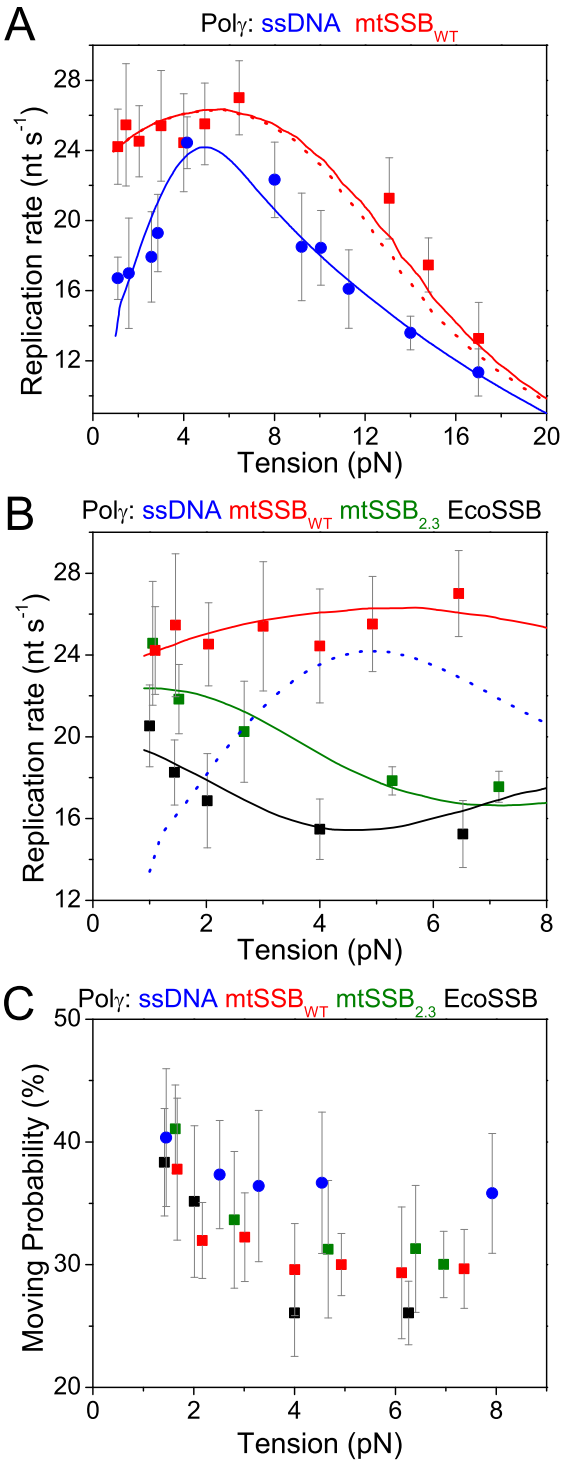

Figure 2. Effect of homologous and non-homologous SSBs on Polγ replication kinetics. (**A**) Change of V_{max} (nt s^{-1}) with tension in SSB-free (blue symbols, $N = 100$) and mtSSB$_{WT}$-covered (red symbols, $N = 109$) ssDNA. Lines represent best fit to data with Equation (1) (solid blue line), Equation (2) (solid red line) and Equation (4) (dotted red line). (**B**) Tension dependence of V_{max} (nt s^{-1}) in ssDNA covered either with mtSSB$_{WT}$ (red symbols), mtSSB$_{2.3}$ (green symbols, $N = 57$) or EcoSSB (black symbols, $N = 30$). Solid lines represent best fit of the data with Equation (4). For reference, dotted blue line shows fit to V_{max} in SSB-free ssDNA (as shown in A). (**C**) Moving probability (average velocity/V_{max}) of Polγ on ssDNA (blue) and on ssDNA covered with mtSSB$_{WT}$ (red), mtSSB$_{2.3}$ (green) and EcoSSB (black). For all figures, error bars show standard errors.

mainly due to disruption of the template secondary structure by tension, while above 6 pN, in the absence of secondary structure ($\varphi(f) = 1$), the replication rate decreases as a result of the work to convert a single- to a double-stranded nucleotide at each tension. Alternative models to interpret the force–velocity behavior of DNA polymerases are discussed in Supplementary Data and Supplementary Figure S7. We note that, although Polγ exhibits both polymerization and proofreading (exonucleolytic) activities *in vitro* and *in vivo*, with our current resolution, we did not detect processive force-induced exonucleolytic activity (FIEA) at any tension below 60 pN, as was previously observed for other DNA polymerases (25,26) (see 'Discussion' section).

Removal of template secondary structure by mtSSB$_{WT}$ increases the instantaneous replication rate by Polγ

Next, we studied the real-time kinetics of individual Polγ holoenzymes in replicating ssDNA covered with mtSSB$_{WT}$ at different template tensions. Analysis of independent replication traces ($N = 109$) showed that the presence of mtSSB$_{WT}$ increased the average replication rate and processivity of Polγ, which is consistent with previous bulk studies (15,48,49). Under these conditions, Polγ replicated the full length of the template, ~900 nt, with an average rate at 1 pN of ~9 nt s^{-1} (Supplementary Figure S5). The presence of mtSSB$_{WT}$ also had a strong effect on $V_{max}(f)$ (Figure 2A): at ~1 pN $V_{max} = 24 \pm 2$ nt s^{-1}, which is the maximum rate measured on free-ssDNA at a tension destabilizing most of the template secondary structure (~6 pN). In addition, below 8 pN, V_{max} presents much weaker force dependence than that measured on free-ssDNA (Figure 2A). These observations suggest that at tensions in which mtSSB$_{WT}$ remains stably bound to ssDNA (<8 pN), its activity in removing the secondary structure of the template (14) plays a key role in stimulating the instantaneous replication rate by Polγ. In fact, the combined effect of tension and mtSSB$_{WT}$ on V_{max} is well explained by the model described above Equation (1), when there is no contribution of the secondary structure of the template, $\varphi(f) \sim 1$ ($k(0)$ was fixed to ~23 nt s^{-1}, by the fit described in the previous section). In other words, in this case, the dependence of V_{max} on tension simply depends on the work to convert in each nucleotide incorporation step ($\delta = 1$) the extension of a SSB-bound nucleotide ($x_{SSB}(f)$) to its double-stranded form ($x_{ds}(f)$). The values of $x_{SSB}(f)$ and $x_{ds}(f)$ were determined experimentally from FECs (Figure 1C); therefore, all parameters of Equation (2) (below) were fixed:

$$V_{max}(f) = k(0)\exp(-[\delta \cdot f \cdot (x_{SSB}(f) - x_{ds}(f))]/k_B T) \quad (2)$$

Regardless of the model used to explain the data, it is striking that mtSSB$_{WT}$ promotes the maximum rate of replication despite its tight association with ssDNA (below 10 pN). This observation suggests strongly the existence of a specific mechanism for 'active' release of mtSSB$_{WT}$ from the template by Polγ.

Table 1. Free-parameters of Equations (1) and (4)

Equation (1) fits to activities in ssDNA			Equation (4) fits to activities in SSB–ssDNA			
	$k(0)$ (nt s^{-1})	ΔG_{eff} (k_BT)		ΔG_{int} (k_BT)	d (nm)	n (nt)
Polγ	23.0 ± 0.7	1.4 ± 0.2	**Polγ-mtSSB$_{WT}$**	−12†	2.7 ± 0.9	1.7 ± 0.4
T7DNAp	90.0 ± 6.0	2.6 ± 0.5	**Polγ-mtSSB$_{2.3}$**	−2.3 ± 0.8	2.6 ± 1.3	1.8 ± 0.3
			Polγ-EcoSSB	−1.0 ± 0.4	2.7 ± 1.2	5.3 ± 1.1
			T7DNAp-mtSSB$_{WT}$	2.2 ± 1.6	2.7*	3.4 ± 0.3
			T7DNAp-EcoSSB	3.5 ± 3.8	2.7*	4.8 ± 0.2

Errors show standard deviations and were estimated with the non-linear regression function of Matlab (nlinfit). †Minimum value of ΔG_{int} fitting experimental data with the least mean squared error (Supplementary Figure S9). *The value of d was set to that obtained from fits with Equation (4) to force–velocity plots of Polγ in mtSSB$_{WT}$- and EcoSSB- ssDNA.

Polymerase–SSB interactions are required for active removal of SSB

In order to characterize the mechanism used by Polγ to displace SSB from the template during DNA synthesis and to determine the putative role of species-specific interactions, we next measured the effect of the human mitochondrial SSB variant mtSSB$_{2,3}$ on the tension-dependent kinetics of Polγ. mtSSB$_{2,3}$ lacks nine residues corresponding to the loop 2,3 (S51– L59), which contribute to the stimulation of the activity of Polγ in bulk but do not influence the affinity of ssDNA binding (17). In fact, under our current experimental conditions, both mtSSB$_{WT}$- and mtSSB$_{2.3}$- ssDNA complexes respond similarly to tension, which is reflected by their nearly identical FECs (Figure 1C).

These experiments were performed at tensions below 8 pN, under which no significant protein detachment is expected, which might complicate data interpretation (14,28). We observed that the replication rate of Polγ on mtSSB$_{2,3}$-DNA presented an entirely different force-dependence from that measured on mtSSB$_{WT}$-DNA complexes ($N = 57$, Figure 2B): at the lowest tension (∼1 pN), V_{max} was similar to that measured with mtSSB$_{WT}$ ($V_{max} = 23 \pm 2$ nt s^{-1}), but it dropped rapidly (by ∼30%) as tension increased to 8 pN, Figure 2B (average replication rates and processivity are shown in Supplementary Figure S5). These results would argue that loop 2.3 plays a key role in the mechanism of SSB displacement from the template by Polγ.

Next, we aimed to check if the measured inhibition of Polγ rate is due to a particular characteristic of the mtSSB$_{2.3}$–DNA complex acquired with application of tension or, instead, is due specifically to the elimination of communication between the two proteins through the loop 2.3. In order to test this possibility, we measured the effect of EcoSSB on the force dependent kinetics of Polγ. EcoSSB represents an ideal model system to test this possibility because of its high degree of sequence, structural and functional homology with mtSSB$_{WT}$ (3,10–14,27,28): both proteins bind to ssDNA as tetramers, with nearly identical binding and apparent dissociation constants, salt dependent binding site-sizes and, they respond similarly to tension on the ssDNA (Figure 1C and Supplementary Figure S2). However, EcoSSB does not contain the equivalent residues corresponding to the loop 2.3 characteristic of animal mitochondrial SSBs. Interestingly, these experiments showed that EcoSSB modulates the force-dependent kinetics of Polγ in a manner very similar to that of mtSSB$_{2.3}$ ($N =$ 30, Figure 2B); at the lowest tension (∼1 pN), V_{max} is equal within error to that measured on mtSSB$_{2,3}$–DNA, $V_{max} = 21 \pm 2$ nt s^{-1}, and decreases rapidly as force increases to ∼8 pN. The characteristic velocity drop with tension, measured for both mtSSB$_{2.3}$ and EcoSSB indicates that a significant conformational change induced by tension hinders the polymerase advance on DNA templates covered with SSBs lacking residues of the loop 2.3.

Overall, the data suggest that specific interactions between Polγ and mtSSB$_{WT}$ mediated by residues of the loop 2.3 prevent the deleterious effect of tension on the replication rate, arguing that these interactions play a crucial role on the mechanism of active release of mtSSB$_{WT}$ from the template by Polγ.

Effect of SSBs on the moving probability of Polγ

In order to estimate the probability to find the polymerase in a pause or moving state during each replication condition, we calculated the moving probability, which was obtained directly from the ratio between the average velocity and V_{max}. Figure 2C shows that the probability of finding Polγ in a moving state while replicating ssDNA was ∼37% and mostly independent of tension below 8 pN. Interestingly, at the lowest tension (∼1 pN) the presence of any of the three tetrameric SSBs under study did not change the moving probability, suggesting that template secondary structure is not the main source of the low moving probability (or high pause occupancy) characteristic of Polγ. Intriguingly, the moving probability decreased by a ∼20% further when replication was measured on ssDNA covered by any of the SSBs at tensions above 2 pN, Figure 2C. This effect suggests that the conformational change induced by tension on the SSB–DNA complexes (see below) also increased the probability of Polγ being in a paused state and/or promoted additional pause state(s). However, proper identification of the type, frequency and length of pauses would be required to interrogate the nature of the high pause occupancy of the mitochondrial polymerase. We note that the method for V_{max} identification presented here ('velocity prominence' method, Supplementary Data) did not allow us to identify pause events directly from individual replication traces.

Determination of interaction energies and conformational changes relevant for SSB displacement

We next sought to determine the magnitude of the conformational change induced by tension on the polymerase–SSB–DNA complexes and to quantify the energetics of

polymerase–SSB interactions required for 'active' SSB release. To this end, we sought the simplest possible model to interpret the different effects of mechanical tension on the replication kinetics of Polγ on the three types of SSB–DNA templates (Supplementary Figure S7). We found that the model described above (Equation 2) explains well the force-dependent replication rate of Polγ on the three SSB covered templates when two additional and contrasting factors are considered:

(i) The probability of the polymerase–SSB complex to establish functional interactions that favor SSB release from ssDNA, $P_{int}(f)$. This probability can be written as:

$$P_{\rm int}(f) = \frac{\exp^{\frac{-(\Delta G_{\rm int} + f \cdot d)}{k_B T}}}{1 + \exp^{\frac{-(\Delta G_{\rm int} + f \cdot d)}{k_B T}}} \quad (3)$$

where ΔG_{int} corresponds to the magnitude of interaction energy between the polymerase–SSB pair that facilitates the release of SSB from the template. ΔG_{int} is compromised by the magnitude of the conformational change induced by tension, *d,* which in turn, would decrease the probability of interaction between Polγ and SSB.

(ii) The average energy barrier to unwrap *n* nucleotides from SSB at each tension, $n{\cdot}\Delta G_{SSB}(f)$, which would hinder polymerase movement. $\Delta G_{SSB}(f)$ was calculated experimentally from the FECs of each SSB–DNA complex ('Materials and Methods' section and Supplementary Figure S2).

Then, V_{max} can be expressed as:

$$V_{\rm max}(f) = k(0) exp\left[-\frac{\delta \cdot f \cdot (x_{\rm SSB}(f) - x_{\rm ds}(f))}{k_B T}\right] \times \left[P_{\rm Int}(f) + (1 - P_{\rm Int}(f)) \exp\left(-\frac{n \cdot \Delta G_{\rm SSB}(f)}{k_B T}\right)\right] \quad (4)$$

The free parameters, ΔG_{int}, *d* and *n*, were fixed by a least squares fit of Equation (4) to experimental data, Figure 2A and B. The values obtained in each case and their corresponding errors are summarized in Table 1. We note that the other parameters of Equation (4) were determined either experimentally or were set by previous fits: $\delta = 1$ nt/ step (42–45), k (0)= 23 nt s^{-1} (fits from Equation (1)), $x_{SSB}(f)$, $x_{ds}(f)$ and $\Delta G_{SSB}(f)$ were determined from experimental FECs (Figure 1C and Supplementary Figure S2D). The results from the fits indicated that an identical tension-induced conformational change, $d \sim 2.7$ nm (Table 1), is compatible with all three situations. The main difference between them lies in the value of the interaction energy between each polymerase–SSB pair, ΔG_{int}. When replication occurs along ssDNA covered with SSBs lacking residues of loop 2.3, the values of ΔG_{int} obtained from the fits were $-2.3 \pm 0.8\ k_B T$ and $-1.0 \pm 0.4\ k_B T$ for $mtSSB_{2.3}$ and EcoSSB, respectively. The combination of relatively low ΔG_{int} and a relatively large conformational change has a strong effect on $P_{int}(f)$, which becomes $<<1$ rapidly with tension (Supplementary Figure S8). Consequently, as the probability of functional interactions between the two proteins decreases, the replication rate decreases concomitantly with the energy barrier imposed by the SSBs, $n{\cdot}\Delta G_{SSB}(f)$. In contrast, when Polγ replicates ssDNA covered with $mtSSB_{WT}$, the least squares fit to data yielded $\Delta G_{int} = -12\ k_B T$ (Table 1 and Supplementary Figure S9). In this case, the magnitude of the interaction is high enough to counterbalance the effect of the conformational change induced by tension, thus ensuring, a high probability of interaction between the two proteins over a wide range of forces, $P_{int}(f) \sim 1$ from 1 to 10 pN (Figure 4 and Supplementary Figure S8). Please note that when $P_{int}(f) \sim 1$, Equation (4) equals Equation (2), and therefore, the replication rate is not hindered by the average energy barrier to unwrap *n* nucleotides from the SSB tetramer, $n{\cdot}\Delta G_{SSB}(f)$. The experimental values of ΔG_{SSB} in the absence of tension, $\Delta G_{SSB}(0)$, were $\sim 0.3\ k_B T$ for both mtSSBs and $\sim 0.18\ k_B T$ for EcoSSB (Supplementary Figure S2D), whereas the values of *n* obtained from the fits were ~2 and ~5 nt for the mitochondrial and *E. coli* SSBs, respectively (see Table 1 and 'Discussion' section).

Effect of homologous and non-homologous SSBs on T7DNAp activity

We sought to understand further the role of catalytically relevant interactions in the mechanism of SSB release by DNA polymerases, and to explore whether the behavior observed for the mitochondrial polymerase can be extended to other DNA replication systems. To this end, we next measured the effect on the instantaneous replication rate of bacteriophage T7 DNA polymerase (T7DNAp) of homologous T7 SSB (gp2.5) and non-homologous ($mtSSB_{WT}$ and EcoSSB) SSB proteins under mechanical tension. Of note is that gp2.5 presents entirely different structural and ssDNA-binding properties than the tetrameric mitochondrial and *E. coli* SSBs used in this study (2). These differences are in part reflected by the FECs of gp2.5–DNA complexes (Figure 1C). First, we characterized the force dependence of the replication kinetics of T7DNAp on ssDNA under the same experimental conditions used for Polγ ('Materials and Methods section'). As reported previously (23,26,50), the replication rate without pauses (V_{max}) of T7DNAp was strongly dependent on tension; it increased rapidly from 1 to 6 pN, decreased toward stalling at tension >6 pN and a strong FIEA prevailed above ~30 pN (Figure 3A and Supplementary Figure S10). As in the case of Polγ, the entire force–velocity behavior of T7DNAp on ssDNA was explained by the model described in Equation ((1) (with $\delta = 1$), which considers the combined effect of tension and template secondary structure on the replication rate (Figure 3A). The values and corresponding errors obtained for the free variables of the model are shown in Table 1.

Next, we measured the activity of T7DNAp on ssDNA templates covered *in situ* by gp2.5, $mtSSB_{WT}$ or EcoSSB at increasing tensions (1–8 pN), and under the same experimental conditions used for Polγ ('Materials and Methods' section). Interestingly, in the presence of the homologous T7 SSB (gp2.5), T7DNAp replicated at $V_{max} \sim 90$ nt s^{-1} at all forces below 6–8 pN (Figure 3B), which is the maximum rate we measured for this polymerase on free-ssDNA at tensions destabilizing most of the template secondary structure (Table 1 and Figure 3A). This behavior was well explained with our model (Equation 4) when the probability of interaction between the two proteins was $P_{int}(f) \sim 1$ (Figure 3B).

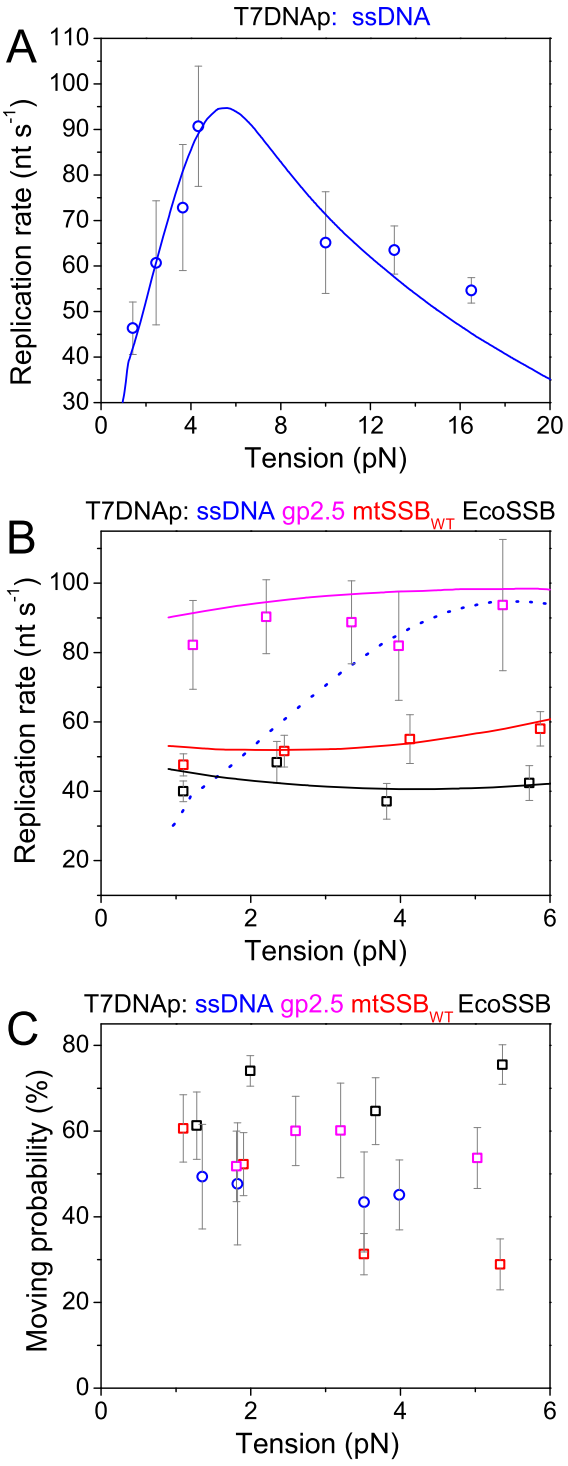

Figure 3. Effect of homologous and non-homologous SSBs on T7DNAp replication kinetics. (**A**) V_{max} (nt s^{-1}) change with tension in SSB-free ssDNA ($N = 42$). Solid line represents best fit to data with Equation (1). (**B**) V_{max} (nt s^{-1}) change with tension on ssDNA covered with gp2.5 ($N = 30$, pink symbols), mtSSB$_{WT}$ ($N = 32$, red symbols) or EcoSSB ($N = 31$, black symbols). Solid lines represent best fits of data with Equation (4): $P_{int}(f)\sim1$ for homologous gp2.5 (magenta) and $P_{int}(f) \sim 0$ for non-homologous mtSSB (red line) and EcoSSB (black line). For comparison, dotted line shows fit to V_{max} of T7DNAp in SSB-free ssDNA (as shown in A). (**C**) Moving probability (average velocity/V_{max}) of T7DNAp on ssDNA (blue) and on ssDNA covered with gp2.5 (magenta), mtSSB$_{WT}$ (red) and EcoSSB (black). For all figures, error bars show standard errors.

Therefore, the effect of gp2.5 on the instantaneous replication kinetics of T7DNAp was comparable to that measured for mtSSB$_{WT}$ on Polγ.

In contrast, in the presence of both non-homologous SSBs (mtSSB$_{WT}$ and EcoSSB), T7DNAp never reached its maximum replication rate; for the full force range under study, V_{max} was found to be identical to that measured in the absence of SSB at the lowest tensions (~45 nt s^{-1} at 1 pN), Figure 3B. Importantly, this behavior was well explained by our model (Equation (4)) when $P_{int}(f) \sim 0$ (Figure 3B). Under these conditions, V_{max} was not stimulated by removal of secondary structure promoted by the SSBs, instead it was hindered by the average energy cost to release n nucleotides from SSB, $n{\cdot}\Delta G_{SSB}(f)$, which again in this case $n \sim 3$ and 5 nt for mtSSB$_{WT}$ and EcoSSB, respectively, were required to explain the experimental data. The absence of interactions relevant for SSB displacement ($P_{int}(f) = 0$) makes these two tetrameric SSBs a barrier to the advancement of T7DNAp. Therefore, the stimulation of T7DNAp replication activity by mtSSB$_{WT}$ (Supplementary Figure S11) and EcoSSB (51,52) observed *in vitro* is likely due to factors other than stimulation of its instantaneous replication rate (see 'Discussion' section).

The moving probability of T7DNAp was not affected by presence of any of the three SSBs at the lowest tensions and seemed fairly independent on tension except for mtSSB$_{WT}$–DNA complexes (Figure 3C). In the latter, the moving probability decreased consistently by a ~50% (from 1 to 6 pN), suggesting that the conformational change induced by tension in the mtSSB$_{WT}$–DNA complexes may, in fact, affect the pause behavior of T7DNAp.

DISCUSSION

SSB proteins provide a platform that allows replicative DNA polymerases to process efficiently ssDNA intermediates generated during DNA replication. To date, the mechanism that is used by replicative polymerases to dislodge the array of tightly bound SSBs to the template remains unclear. The high density of SSB bound to the template would restrict the capacity of a single SSB to diffuse. In addition, the absence of free ssDNA ends in replicative intermediates prevents SSB from being pushed off by the advance of the lagging strand polymerase. Therefore, an active mechanism for SSB release would be expected so that SSB does not compromise the advance of the replication fork. In order to interrogate this mechanism, we have measured the combined effect of mechanical tension and SSB on the instantaneous replication rate (V_{max}) of Polγ and T7DNAp, in a single molecule assay that mimics lagging strand synthesis.

Analysis of FECs of ssDNA and SSB–DNA complexes provided the average distance per nucleotide in each case (required for data analysis, Figure 1C)) and indicated that, under current experimental conditions, the tetrameric SSBs bind to ssDNA in the low site-size mode (Supplementary Figure S2), which has been proposed as the relevant binding mode for DNA replication (14). Next, we showed that the marked effect of tension on V_{max} of Polγ and T7DNAp can be explained readily by a model in which the replication rate is modulated by the work to convert a single- to a double-stranded nucleotide at each tension plus the work to

unravel the secondary structure characteristic of ssDNA at low tensions (Equation (1)). As for the majority of replicative DNA polymerases, the *in vitro* activities of Polγ and T7DNAp are hampered by the secondary structure of the template. Accordingly, V_{max} increases rapidly as tension disrupts the secondary structure of the template and peaks at those tensions, ∼6 pN, promoting the full destabilization of various possible configurations that characterize the condensed phase of the ssDNA at low forces under our experimental conditions (Supplementary Figure S3). Above 6 pN, in the absence of secondary structure, the replication rate decreases with the work to convert a single- to a double-stranded nucleotide at increasing tensions. Interestingly, the results from the fits indicated that the average effective energy barrier imposed by the template secondary structure to the advance of the polymerase, ΔG_{eff}, is significantly greater for T7DNAp, $\Delta G_{eff} \sim 2.6\ k_BT$, than for Polγ $\Delta G_{eff} \sim 1.4\ k_BT$ (Table 1). This difference suggests an enhanced ability of the mitochondrial DNA polymerase to cope with the high configurational entropy characteristic ssDNA at low forces. Other alternative models have been used to explain similar force–velocity dependencies of other DNA polymerases replicating on ssDNA (23,26,53–55 and discussed in Supplementary Data). In contrast with these models, the major strengths of our model are: (i) it is based on measurable experimental observations (does not require assumptions regarding the nature of rate-limiting steps or polymerase–DNA organizations) and (ii) it fits well the entire data set with a kinetic step size of $\delta = 1$ nt, in full agreement with previous biochemical, structural and single-molecule observations (42–45). Future single-molecule manipulation experiments, which should quantify the amount of secondary structure of the template, will help to test the efficacy of our model and of alternative models to explain the force-dependent rate of different replicative DNA polymerases.

Notably, we did not detect processive FIEA at any tension below 60 pN for Polγ, which contrasts with the fast (∼200 nt s^{-1}) FIEA observed here and in previous studies for T7DNAp at forces >30 pN, Supplementary Figure S10 (26,50). We suspect that the slow exonucleolytic rate of Polγ on ssDNA, which is $>10^3$ times slower than that of T7DNAp (46), either prevents FIEA to occur or deters its detection with our current resolution. In spite of its slow exonucleolytic rate, Polγ presents a high intrinsic fidelity of replication, $\sim 2 \times 10^{-6}$, and very low probability of excision of a correctly base paired nucleotide (∼0.14%) (46,47). This suggests strongly that the occurrence of single exonucleolytic events, which would be detected as pauses under our experimental conditions, are highly improbable and thus, other factors are likely responsible for the low moving probability, 37%, (or high pause occupancy) measured for this polymerase (Figure 2C). However, as mentioned before, a detailed identification of the type and characteristics of pause events would be required to reveal their nature.

For both DNA polymerases, the presence of SSB had a marked effect on V_{max} and its response to tension (Figures 2 and 3). In the presence of their homologous SSBs, Polγ and T7DNAp replicated at their maximum rates at all tensions <8 pN. In contrast, non-homologous SSBs presented a barrier for the advance of both polymerases, slowing down their $V_{max}(f)$, although in slightly different ways. Regarding the magnitude of this barrier ($n \cdot \Delta G_{SSB}(f)$), our data indicated that $n \sim 2$–3 and 5 nucleotides are unwrapped from mtSSB and EcoSSB, respectively, in each nucleotide incorporation step by Polγ and T7DNAp (Table 1). These differences may suggest the existence of significant variations in the way ssDNA is unwrapped from SSBs of different origin. However, the energy to unwrap a single nucleotide from mtSSB is higher than that for EcoSSB, $\Delta G_{SSB}(0) \sim 0.3\ k_BT$ versus $0.18\ k_BT$, respectively (Supplementary Figure S2D; 14,27,28). Therefore, the energy barrier imposed by the mitochondrial (wild-type and variant) and *E. coli* SSB proteins to the advance of Polγ and T7DNAp at zero tension is $n \cdot \Delta G_{SSB}(0) \sim 1\ k_BT$ per nucleotide incorporation step.

According to our model (Equation 4), functional interactions between polymerase and SSB must be established so that the energy barrier of ssDNA unwrapping from the SSB does not slow down the replication rate. As shown in Equation (3), the probability to establish these functional interactions, $P_{int}(f)$, depends on the magnitude of the interaction energy between the polymerase and the SSB, ΔG_{int}, and on the magnitude of the tension-induced conformational change in the SSB–DNA complex, d. The evidence for a conformational change come from the gradual decrease of V_{max} with tension observed for Polγ when replicating on ssDNA covered by $mtSSB_{2.3}$ and EcoSSB. Importantly, a conformational change of $d \sim 2.7$ nm explained well all V_{max} dependencies on tension measured when replication occurred along ssDNA covered by the mitochondrial and *E. coli* SSB proteins. This result would reflect the similarity of the ssDNA-binding properties (and their response to tension) of the tetrameric SSBs, and suggests strongly that the tension-induced conformational change mainly affects the SSB–DNA complex. According to recent single-molecule and molecular dynamics simulations studies, stretching a single ssDNA–EcoSSB complex below 8 pN aligns the SSB tetramer along the pulling coordinate and favors the unwrapping of several nucleotides from the SSB ends (28,56). For example, considering an average distance per ssDNA nucleotide within the 1–8 pN range of ∼0.3 nm/nt, the unwrapping of ∼3 nt from each side of the SSB tetramer [(3 nt × 0.3 nm/nt) × 2 = 1.8 nm] plus tilting of the mtSSB tetramer along its longer axis ($mtSSB_{WT}$ and EcoSSB dimensions ∼8 × 4 nm (10, 11)) could easily account for the ∼2.7 nm conformational change obtained from fits to the data. Note that this conformational change implies a reorganization of the SSB–DNA complex and does not necessarily imply a physical separation between the polymerase and the SSB by 3 nm (Figure 4). Importantly, this conformational change does not inhibit the replication rate of Polγ on $mtSSB_{WT}$–DNA and does not further decrease the replication rate of T7DNAp in EcoSSB- or $mtSSB_{WT}$-covered ssDNA. These results argue that the conformational change induced by tension on the SSB–DNA complex does not generate an artifactual barrier for polymerase progression; instead, it affects specifically the likelihood to establish functional interactions between the polymerase and the SSB relevant for SSB displacement, $P_{int}(f)$ (see below).

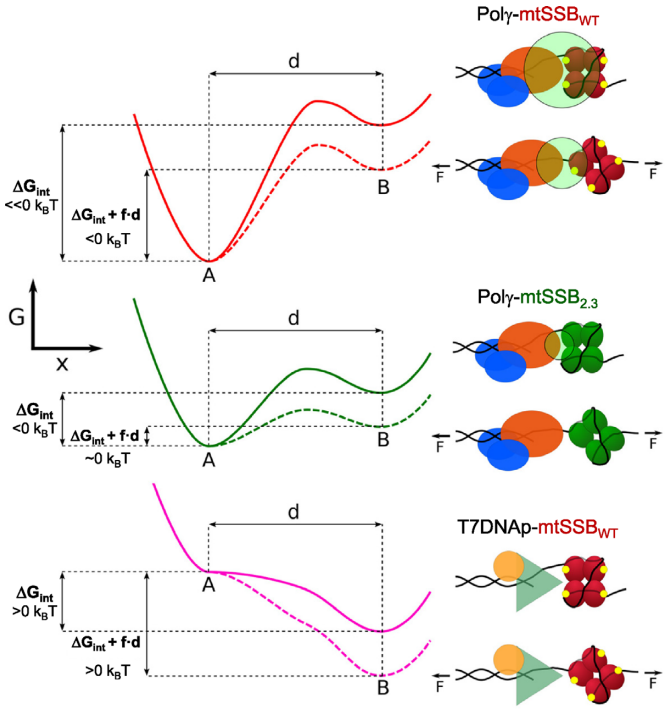

Figure 4. Model interpretation. (Left) Notional energy landscapes that connect interaction (**A**) and non-interaction states (**B**) of Pol-SSB complexes with the reaction coordinate, *x*, corresponding to the conformational change induced by tension, *d*. Colored solid and dotted lines represent energy landscapes before and after tension (*F*) application, respectively. (Right) Conceptual diagrams for the most probable organization of Pol−SSB complexes in each case. For the homologous Polγ-mtSSB$_{WT}$ couple (Top), the electrostatic repulsion between the negatively-charged surface of the catalytic subunit of the polymerase (red) and the negatively-charged residues of the loop 2.3 of mtSSB$_{WT}$ (yellow dots) ensures high interaction energy between the two proteins, $\Delta G_{int} \sim -12\ k_BT$. The magnitude of ΔG_{int} is such that it ensures a high probability of functional interactions (green circle) between the two proteins, even under stress conditions (such as *F)* that may affect the overall organization of the mtSSB$_{WT}$–ssDNA complex (P_{int}(0–8 pN) ∼ 1; Supplementary Figure S8). This interaction favors the displacement of mtSSB$_{WT}$ from the template under a wide range of forces. For the Polγ-mtSSB$_{2.3}$ couple (Center), the absence of negatively-charged residues of loop 2.3 decreases markedly the interaction energy between the two proteins to $\Delta G_{int} \sim -2\ k_BT$ and concomitantly, their probability of interaction (green circle). In this case, an external factor affecting further the communication between them, such as the conformational change (*d*) induced by tension, would decrease rapidly $P_{int}(f)$ <<1 (Supplementary Figure S8), and the replication rate would decrease concomitantly with the energy barrier to unwrap *n* nucleotides from the SSB tetramer. For non-homologous Pol-SSB systems (Bottom), such as T7DNAp-mtSSB$_{WT}$, functional interactions are already disfavored in the absence of tension (Table 1), implying a null probability to establish functional interactions, $P_{int}(f) \sim 0$ (Supplementary Figure S8), which could facilitate the release of SSB.

The main differences accounting for the particular force–velocity dependence of each polymerase–SSB complex rely on the interaction energies between the two proteins, ΔG_{int}. For Polγ when replication occurs in the presence of its homologous mtSSB$_{WT}$, $\Delta G_{int} \sim -12\ k_BT$. This high interaction energy ensures a high probability of interaction between the two proteins, $P_{int}(f) \sim 1$, for a wide range of tensions (Figure 4 and Supplementary Figure S8). This would allow Polγ to overcome the energetic barrier imposed by the high binding affinity of mtSSB to ssDNA and to remove actively the mtSSB tetramer from the ssDNA even at tensions that disrupt the original conformation of the mtSSB–DNA complex (<8 pN). In this way, the polymerase would replicate at its maximum rate in a template free of secondary structure. Similarly, $P_{int}(f) \sim 1$ explains nicely the effect of bacteriophage T7 SSB (gp2.5) on the replication rate of its homologous polymerase. This argues for high interaction energy between these two proteins, which in turn enables T7DNAp to replicate at its maximum rate along the gp2.5 covered ssDNA template. Future studies to determine the average energy to unwrap a single nucleotide from gp2.5 ($\Delta G_{SSB}(f)$) would be required for an accurate quantification of the interaction energy between these two proteins.

In contrast, the lower interaction energies between non-homologous polymerase–SSB couples modulated differently the observed response of V_{max} with tension. On one hand, for Polγ, the interaction energies with mtSSB$_{2.3}$ and EcoSSB are about 6 to 12 times lower, $\Delta G_{int} \sim -2\ k_BT$ and $-1\ k_BT$ respectively, than that of Polγ with its homologous mtSSB$_{WT}$ (Table 1). Under these conditions, the probabilities to establish functional interactions are still significant at the lowest tensions (Supplementary Figure S8). However, the lower ΔG_{int} values make the probabilities of interaction more sensitive to external factors, such as external tension and therefore, to decrease rapidly due to the conformational change induced by tension on the SSB–DNA complex (Figure 4 and Supplementary Figure S8). As the probabilities to establish functional interactions decrease, the replication rates are slowed down concomitantly by the effective energy barrier imposed by each SSB tetramer, $n \cdot \Delta G_{SSB}(f)$. On the other hand, the interaction energies of T7DNAp with the non-homologous mtSSB$_{WT}$ and EcoSSB proteins are completely disfavored (Table 1), implying therefore, a null probability to establish functional interactions, $P_{int}(f) \sim 0$ (Supplementary Figure S8). In the absence of functional interactions, these tetrameric SSBs constitute a barrier for the advance of T7DNAp, slowing down its V_{max} even at the lowest tensions (Figure 3B).

Overall, our results support a mechanism in which SSB promotes the maximum replication rate of the lagging strand polymerase indirectly, by elimination of the secondary structure of the template. However, for this to occur, an interaction energy between the polymerase/SSB pair is required to overcome the energy of binding of SSB to ssDNA and for the polymerase to dislodge actively the SSB from ssDNA. At present, our data do not reveal the nature of polymerase–SSB interactions required for active SSB release. Physical interactions between mtSSB and proteins involved in DNA repair have been shown (57,58), but there is no evidence to date of direct physical interactions between Polγ and mtSSB. In contrast, T7DNAp is known to interact physically with the C-terminal tails of the homologous gp2.5 SSB and non-homologous EcoSSB (2,59). However, our data show that this interaction is not sufficient for the active displacement of EcoSSB, as this tetrameric SSB prevents T7DNAp from reaching its maximum replication rate (Figure 3B). These observations suggest that instead of (or in addition to) physical interactions, other types of interactions would modulate the communication between homologous polymerase–SSB couples, which is required for proper synthesis of the lagging strand. In consideration of

this and previous studies (59), we support a mechanism in which the nature of the interaction energy between the polymerase and the SSB required for active SSB release during lagging DNA synthesis involves repulsive electrostatic interactions. In the case of the mitochondrial DNA replication system, these may result from interactions of negatively-charged residues (S51, S54, Y57, D53, 55E and Q58) within each of the four loops 2.3 (one per monomer) that are located at the surface of mtSSBs, and the significantly net negative charge of the catalytic subunit of Polγ (isoelectric point ∼6.15 under our experimental conditions, pH 8.5). Interestingly, the ability of Polγ to displace actively $mtSSB_{2.3}$ and EcoSSB at the lowest tension (∼1 pN) suggests that additional residues, other than those of loop 2.3, play lesser, although significant, roles in the interaction between the two proteins. However, these are apparently not sufficiently robust to overcome the energy barrier to release SSB either under stress or changing physiological conditions. Based on the similarities found between the human mitochondrial and bacteriophage T7 DNA replication systems (comprising SSBs from different origin and with different structural and biochemical properties), it is tempting to speculate that other eukaryotic and prokaryotic DNA replication systems may use similar mechanisms of SSB displacement by replicative DNA polymerases during lagging strand DNA synthesis.

SUPPLEMENTARY DATA

Supplementary Data are available at NAR Online.

ACKNOWLEDGEMENTS

We are grateful to Dr J. Jarillo for helping with data analysis and to members of B. Ibarra lab for useful discussions.

FUNDING

Spanish Ministry of Economy and Competitiveness [FIS2015–67765-R to F.J.C., BFU2012–31825, BFU2015–63714-R to B.I.]; National Institutes of Health [GM45925 to L.S.K.]; Comunidad de Madrid [NanoMagCOST P2018 INMT-4321]; Programa de Financiación Universidad Complutense de Madrid–Santander Universidades [CT45/15-CT46/15 to F.C.]; Ministerio de Educación Cultura y Deporte [FPU2014/06867 to K.M.L.]; IMDEA Nanociencia acknowledges support from the 'Severo Ochoa' Programme for Centers of Excellence in R&D [MINECO, Grant SEV-2016–0686]. Funding for open access charge: Spanish Ministry of Economy and Competitiveness [BFU2015-63714-R].
Conflict of interest statement. None declared.

REFERENCES

1. Antony,E. and Lohman,T.M. (2018) Dynamics of E. coli single stranded DNA binding (SSB) protein-DNA complexes. *Semin. Cell Dev. Biol.*, **86**, 102–111.
2. Hernandez,A.J. and Richardson,C.C. (2018) Gp2.5, the multifunctional bacteriophage T7 single-stranded DNA binding protein. *Semin. Cell Dev. Biol.*, **86**, 92–101.
3. Lohman,T.M. and Ferrari,M.E. (1994) Escherichia Coli Single-Stranded DNA-Binding Protein: Multiple DNA-Binding modes and cooperativities. *Annu. Rev. Biochem.*, **63**, 527–570.
4. Shereda,R.D., Kozlov,A.G., Lohman,T.M., Cox,M.M. and Keck,J.L. (2008) SSB as an Organizer/Mobilizer of genome maintenance complexes. *Crit. Rev. Biochem. Mol. Biol.*, **43**, 289–318.
5. Brown,T.A., Cecconi,C., Tkachuk,A.N., Bustamante,C. and Clayton,D.A. (2005) Replication of mitochondrial DNA occurs by strand displacement with alternative light-strand origins, not via a strand-coupled mechanism. *Genes Dev.*, **19**, 2466–2476.
6. Graziewicz,M.A., Longley,M.J. and Copeland,W.C. (2006) DNA polymerase γ in mitochondrial DNA replication and repair. *Chem. Rev.*, **106**, 383–405.
7. Gustafsson,C.M., Falkenberg,M. and Larsson,N.-G. (2016) Maintenance and expression of mammalian mitochondrial DNA. *Annu. Rev. Biochem.*, **85**, 133–160.
8. Miralles Fusté,J., Shi,Y., Wanrooij,S., Zhu,X., Jemt,E., Persson,Ö., Sabouri,N., Gustafsson,C.M. and Falkenberg,M. (2014) In vivo occupancy of mitochondrial single-stranded DNA binding protein supports the strand displacement mode of DNA replication. *PLoS Genet.*, **10**, e1004832.
9. Phillips,A.F., Millet,A.R., Tigano,M., Dubois,S.M., Crimmins,H., Babin,L., Charpentier,M., Piganeau,M., Brunet,E. and Sfeir,A. (2017) Single-Molecule analysis of mtDNA replication uncovers the basis of the common deletion. *Mol. Cell*, **65**, 527–538.
10. Raghunathan,S., Kozlov,A.G., Lohman,T.M. and Waksman,G. (2000) Structure of the DNA binding domain of E. coli SSB bound to ssDNA. *Nat. Struct. Mol. Biol.*, **7**, 648–652.
11. Yang,C., Curth,U., Urbanke,C. and Kang,C. (1997) Crystal structure of human mitochondrial single-stranded DNA binding protein at 2.4 Å resolution. *Nat. Struct. Mol. Biol.*, **4**, 153–157.
12. Kaur,P., Longley,M.J., Pan,H., Wang,H. and Copeland,W.C. (2018) Single-molecule DREEM imaging reveals DNA wrapping around human mitochondrial single-stranded DNA binding protein. *Nucleic Acids Res.*, **46**, 11287–11302.
13. Qian,Y. and Johnson,K.A. (2017) The human mitochondrial single-stranded DNA-binding protein displays distinct kinetics and thermodynamics of DNA binding and exchange. *J. Biol. Chem.*, **292**, 13068–13084.
14. Morin,J.A., Cerrón,F., Jarillo,J., Beltran-Heredia,E., Ciesielski,G.L., Arias-Gonzalez,J.R., Kaguni,L.S., Cao,F.J. and Ibarra,B. (2017) DNA synthesis determines the binding mode of the human mitochondrial single-stranded DNA-binding protein. *Nucleic Acids Res.*, **45**, 7237–7248.
15. Ciesielski,G.L., Bermek,O., Rosado-Ruiz,F.A., Hovde,S.L., Neitzke,O.J., Griffith,J.D. and Kaguni,L.S. (2015) Mitochondrial single-stranded DNA-binding proteins stimulate the activity of DNA polymerase γ by organization of the template DNA. *J. Biol. Chem.*, **290**, 28697–28707.
16. Farr,C.L., Wang,Y. and Kaguni,L.S. (1999) Functional interactions of mitochondrial DNA polymerase and single-stranded DNA-binding protein: template-primer DNA binding and initiation and elongation of DNA strand synthesis. *J. Biol. Chem.*, **274**, 14779–14785.
17. Oliveira,M.T. and Kaguni,L.S. (2011) Reduced stimulation of recombinant DNA polymerase γ and mitochondrial DNA (mtDNA) helicase by variants of mitochondrial single-stranded DNA-binding protein (mtSSB) correlates with defects in mtDNA replication in animal cells. *J. Biol. Chem.*, **286**, 40649–40658.
18. Roy,R., Kozlov,A.G., Lohman,T.M. and Ha,T. (2009) SSB protein diffusion on single-stranded DNA stimulates RecA filament formation. *Nature*, **461**, 1092–1097.
19. Zhou,R., Kozlov,A.G., Roy,R., Zhang,J., Korolev,S., Lohman,T.M. and Ha,T. (2011) SSB functions as a sliding platform that migrates on DNA via reptation. *Cell*, **146**, 222–232.
20. Sokoloski,J.E., Kozlov,A.G., Galletto,R. and Lohman,T.M. (2016) Chemo-mechanical pushing of proteins along single-stranded DNA. *Proc. Natl. Acad. Sci. U.S.A.*, **113**, 6194–6199.
21. Ibarra,B., Chemla,Y.R., Plyasunov,S., Smith,S.B., Lázaro,J.M., Salas,M. and Bustamante,C. (2009) Proofreading dynamics of a processive DNA polymerase. *EMBO J.*, **28**, 2794–2802.
22. Kim,S., Schroeder,C.M. and Xie,X.S. (2010) Single-Molecule study of DNA polymerization activity of HIV-1 reverse transcriptase on DNA templates. *J. Mol. Biol.*, **395**, 995–1006.

23. Maier,B., Bensimon,D. and Croquette,V. (2000) Replication by a single DNA polymerase of a stretched single-stranded DNA. *Proc. Natl. Acad. Sci. U.S.A.*, **97**, 12002–12007.
24. Manosas,M., Spiering,M.M., Ding,F., Bensimon,D., Allemand,J.-F., Benkovic,S.J. and Croquette,V. (2012) Mechanism of strand displacement synthesis by DNA replicative polymerases. *Nucleic Acids Res.*, **40**, 6174–6186.
25. Naufer,M.N., Murison,D.A., Rouzina,I., Beuning,P.J. and Williams,M.C. (2017) Single-molecule mechanochemical characterization of E. coli pol III core catalytic activity. *Protein Sci.*, **26**, 1413–1426.
26. Wuite,G.J.L., Smith,S.B., Young,M., Keller,D. and Bustamante,C. (2000) Single-molecule studies of the effect of template tension on T7 DNA polymerase activity. *Nature*, **404**, 103.
27. Bell,J.C., Liu,B. and Kowalczykowski,S.C. (2015) Imaging and energetics of single SSB-ssDNA molecules reveal intramolecular condensation and insight into RecOR function. *eLife*, **4**, e08646.
28. Suksombat,S., Khafizov,R., Kozlov,A.G., Lohman,T.M. and Chemla,Y.R. (2015) Structural dynamics of E. coli single-stranded DNA binding protein reveal DNA wrapping and unwrapping pathways. *eLife*, **4**, e08193.
29. Oliveira,M.T. and Kaguni,L.S. (2009) In: Stuart,JA (ed). *Mitochondrial DNA: Methods and Protocols*. Humana Press, Totowa, NJ, pp. 37–58.
30. Smith,S.B., Cui,Y. and Bustamante,C. (2003) Optical-trap force transducer that operates by direct measurement of light momentum. *Methods Enzymol.*, **361**, 134–162.
31. Morin,J.A., Cao,F.J., Lázaro,J.M., Arias-Gonzalez,J.R., Valpuesta,J.M., Carrascosa,J.L., Salas,M. and Ibarra,B. (2012) Active DNA unwinding dynamics during processive DNA replication. *Proc. Natl. Acad. Sci. U.S.A.*, **109**, 8115–8120.
32. Bosco,A., Camunas-Soler,J. and Ritort,F. (2014) Elastic properties and secondary structure formation of single-stranded DNA at monovalent and divalent salt conditions. *Nucleic Acids Res.*, **42**, 2064–2074.
33. Jarillo,J., Morín,J.A., Beltrán-Heredia,E., Villaluenga,J.P.G., Ibarra,B. and Cao,F.J. (2017) Mechanics, thermodynamics, and kinetics of ligand binding to biopolymers. *PLoS ONE*, **12**, e0174830.
34. Smith,S.B., Cui,Y. and Bustamante,C. (1996) Overstretching B-DNA: The elastic response of individual Double-Stranded and Single-Stranded DNA molecules. *Science*, **271**, 795–799.
35. Fan,L., Kim,S., Farr,C.L., Schaefer,K.T., Randolph,K.M., Tainer,J.A. and Kaguni,L.S. (2006) A novel processive mechanism for DNA synthesis revealed by structure, modeling and mutagenesis of the accessory subunit of human mitochondrial DNA polymerase. *J. Mol. Biol.*, **358**, 1229–1243.
36. Kaguni,L.S. (2004) DNA polymerase γ, the mitochondrial replicase. *Annu. Rev. Biochem.*, **73**, 293–320.
37. Dulin,D., Vilfan,I.D., Berghuis,B.A., Hage,S., Bamford,D.H., Poranen,M.M., Depken,M. and Dekker,N.H. (2015) Elongation-competent pauses govern the fidelity of a viral RNA-dependent RNA polymerase. *Cell Rep.*, **10**, 983–992.
38. Hacker,K.J. and Alberts,B.M. (1994) The rapid dissociation of the T4 DNA polymerase holoenzyme when stopped by a DNA hairpin helix. A model for polymerase release following the termination of each Okazaki fragment. *J. Biol. Chem.*, **269**, 24221–24228.
39. Johnson,A. and O'Donnell,M. (2005) Cellular DNA Replicases: Components and dynamics at the replication fork. *Annu. Rev. Biochem.*, **74**, 283–315.
40. Kaguni,L.S. and Clayton,D.A. (1982) Template-directed pausing in in vitro DNA synthesis by DNA polymerase a from Drosophila melanogaster embryos. *Proc. Natl. Acad. Sci. U.S.A.*, **79**, 983–987.
41. Bustamante,C., Chemla,Y.R., Forde,N.R. and Izhaky,D. (2004) Mechanical processes in biochemistry. *Annu. Rev. Biochem.*, **73**, 705–748.
42. Berman,A.J., Kamtekar,S., Goodman,J.L., Lázaro,J.M., de Vega,M., Blanco,L., Salas,M. and Steitz,T.A. (2007) Structures of phi29 DNA polymerase complexed with substrate: the mechanism of translocation in B-family polymerases. *EMBO J.*, **26**, 3494–3505.
43. Li,Y., Korolev,S. and Waksman,G. (1998) Crystal structures of open and closed forms of binary and ternary complexes of the large fragment of Thermus aquaticus DNA polymerase I: structural basis for nucleotide incorporation. *EMBO J.*, **17**, 7514–7525.
44. Morin,J.A., Cao,F.J., Lázaro,J.M., Arias-Gonzalez,J.R., Valpuesta,J.M., Carrascosa,J.L., Salas,M. and Ibarra,B. (2015) Mechano-chemical kinetics of DNA replication: identification of the translocation step of a replicative DNA polymerase. *Nucleic Acids Res.*, **43**, 3643–3652.
45. Pandey,M. and Patel,S.S. (2014) Helicase and polymerase move together close to the fork junction and copy DNA in one-nucleotide steps. *Cell Rep.*, **6**, 1129–1138.
46. Lee,H.R. and Johnson,K.A. (2006) Fidelity of the human mitochondrial DNA polymerase. *J. Biol. Chem.*, **281**, 36236–36240.
47. Johnson,A.A. and Johnson,K.A. (2001) Exonuclease proofreading by human mitochondrial DNA polymerase. *J. Biol. Chem.*, **276**, 38097–38107.
48. Williams,A.J. and Kaguni,L.S. (1995) Stimulation of Drosophila mitochondrial DNA polymerase by single-stranded DNA-binding protein. *J. Biol. Chem.*, **270**, 860–865.
49. Korhonen,J.A., Pham,X.H., Pellegrini,M. and Falkenberg,M. (2004) Reconstitution of a minimal mtDNA replisome in vitro. *EMBO J.*, **23**, 2423–2429.
50. Hoekstra,T.P., Depken,M., Lin,S.-N., Cabanas-Danés,J., Gross,P., Dame,R.T., Peterman,E.J.G. and Wuite,G.J.L. (2017) Switching between exonucleolysis and replication by T7 DNA polymerase ensures high fidelity. *Biophys. J.*, **112**, 575–583.
51. Myers,T.W. and Romano,L.J. (1988) Mechanism of stimulation of T7 DNA polymerase by Escherichia coli single-stranded DNA binding protein (SSB). *J. Biol. Chem.*, **263**, 17006–17015.
52. Nakai,H. and Richardson,C.C. (1988) The effect of the T7 and Escherichia coli DNA-binding proteins at the replication fork of bacteriophage T7. *J. Biol. Chem.*, **263**, 9831–9839.
53. Andricioaei,I., Goel,A., Herschbach,D. and Karplus,M. (2004) Dependence of DNA polymerase replication rate on external Forces: A model based on molecular dynamics simulations. *Biophys. J.*, **87**, 1478–1497.
54. Goel,A., Frank-Kamenetskii,M.D., Ellenberger,T. and Herschbach,D. (2001) Tuning DNA "strings": Modulating the rate of DNA replication with mechanical tension. *Proc. Natl. Acad. Sci. U.S.A.*, **98**, 8485–8489.
55. Nong,E.X., DeVience,S.J. and Herschbach,D. (2012) Minimalist model for Force-Dependent DNA replication. *Biophys. J.*, **102**, 810–818.
56. Maffeo,C. and Aksimentiev,A. (2017) Molecular mechanism of DNA association with single-stranded DNA binding protein. *Nucleic Acids Res.*, **45**, 12125–12139.
57. Sharma,N., Chakravarthy,S., Longley,M.J., Copeland,W.C. and Prakash,A. (2018) The C-terminal tail of the NEIL1 DNA glycosylase interacts with the human mitochondrial single-stranded DNA binding protein. *DNA Repair*, **65**, 11–19.
58. Wong,T.S., Rajagopalan,S., Townsley,F.M., Freund,S.M., Petrovich,M., Loakes,D. and Fersht,A.R. (2009) Physical and functional interactions between human mitochondrial single-stranded DNA-binding protein and tumour suppressor p53. *Nucleic Acids Res.*, **37**, 568–581.
59. Ghosh,S., Hamdan,S.M. and Richardson,C.C. (2010) Two modes of interaction of the single-stranded DNA-binding protein of bacteriophage T7 with the DNA polymerase-thioredoxin complex. *J. Biol. Chem.*, **285**, 18103–18112.